On the Separability of Beamforming for Reconfigurable Intelligent Surfaces under Statistical CSI

Maryam Farahnak-Ghazani, Negar Daryanavardan, and Aria Nosratinia
The University of Texas at Dallas, Richardson, Texas, USA
Email: {maryam.farahnak, negar.daryanavardan, aria} @utdallas.edu

2024 IEEE International Symposium on Information Theory (ISIT) | 979-8-3503-8284-6/24/$31.00 ©2024 IEEE | DOI: 10.1109/ISIT57864.2024.10619291

***Abstract*—Reconfigurable Intelligent Surfaces (RIS) have channel models with many parameters, motivating the study and use of statistical channel state information (CSI) in this context. This paper investigates the question of separability of RIS/transmitter beamforming under spatially correlated Rician fading with statistical channel state information. Subject to any spatial correlation, as long as the transmitter-RIS channel is Rayleigh, we show that the beamforming optimization decomposes into two independent optimizations involving the RIS correlation matrix, and the transmitter array correlation matrix. The tools and techniques of this paper also lead to novel and useful optimizations for beamforming optimization when the transmitter-RIS channel is Rician with non-zero mean, even though in this case separability is not established. Numerical results support our findings and provide insights into the proposed algorithm.**

***Index Terms*—Reconfigurable intelligent surface (RIS), statistical CSI, spatially-correlated Rician and Rayleigh fading,**

I. Introduction

In reconfigurable intelligent surface (RIS) aided channels [1]–[3], beamforming algorithms often require instantaneous channel state information (CSI), which imposes a large overhead [4]. The amount of training overhead required can limit the useful size of RIS arrays [5]. To take advantage of larger RIS arrays, one suggested approach is to rely on statistical (rather than instantaneous) CSI [6]. Joint design of transmitter and RIS beamforming under statistical CSI is considered in [6]–[9], where iterative algorithms have been used to optimize beamforming. The case of statistical CSI for the RIS *but* instantaneous CSI for the transmitter is studied in [10]–[12].

This paper studies the question of the separability of beamforming in RIS/transmitter under spatially correlated channels with statistical CSI. We show that when the channel from the transmitter to RIS is Rayleigh distributed (and the other links are either Rayleigh or Rician), the best joint optimization of beamforming is achieved via cost functions that are local to the transmitter and to RIS, respectively. The tools and techniques developed in this paper also yield new and useful results for beamforming when the transmitter-RIS link is Rician with a non-zero mean, even though in that case separability is not established.

This work was supported in part by the grants 1956213 and 2148211 from the National Science Foundation.

The question of separability was considered in [9] in the asymptotic regime of infinite RIS elements with finite per-element reflection power, using signal-to-interference-and noise ratio (SINR) expressions to calculate multi-user downlink sum-rates. However, under the model employed in [9] with infinite-size RIS, single-user achievable rates would be infinite, therefore *time-sharing* multi-user rates are infinite too. As a result, the interference-as-noise multi-user lower bound utilized in [9] is infinitely loose, and the results are unuseful.[1]

Our separability result is revealed via a careful decomposition of the signal-to-noise ratio (SNR) under the Kronecker model for correlated Rician and Rayleigh fading. Under Rayleigh fading for the transmitter-RIS link, the decomposition naturally leads to a locality/separability result that has not been evident in previous works. To be specific, in this case, RIS beamforming uses only the RIS correlation matrix, and transmit beamforming only uses the correlation matrix of the transmitter array. When the transmitter-RIS link is Rician with a non-zero mean, we do not establish separability but produce new and efficient expressions for the iterative optimization of beamforming. We characterize RIS beamforming optimization via convex relaxation and semidefinite methods. Numerical results validate our findings and illustrate the effectiveness of the proposed passive and active beamforming designs in terms of the ergodic capacity.

II. System Model

We consider a narrowband point-to-point communication system assisted by an RIS. The transmitter (Tx) consists of M_{t} antennas, communicating with the receiver (Rx) equipped with M_{r} antennas, through the RIS with N controllable elements. For brevity, it is assumed that the direct link between the Tx and the Rx is absent, and they only communicate through the RIS. Let $\mathbf{G} \in \mathbb{C}^{N\times M_{\mathrm{t}}}$ and $\mathbf{H} \in \mathbb{C}^{M_{\mathrm{r}}\times N}$ denote the Tx-RIS channel and the RIS-Rx channel, respectively. The received signal at the Rx at each time interval, $\mathbf{y} \in \mathbb{C}^{M_{\mathrm{r}}\times 1}$, is written as follows:

$$\mathbf{y} = \sqrt{\rho}\mathbf{H}\mathbf{\Phi}\mathbf{G}\mathbf{f}x + \mathbf{z}, \tag{1}$$

where $\mathbf{f} \in \mathbb{C}^{M_{\mathrm{t}}\times 1}$ is the beamforming vector, $x \in \mathbb{C}$ is the transmitted signal with $\mathbb{E}[|x|^2] = 1$, and ρ is the total transmit

[1] Also, [9] establishes successive optimization at RIS and transmitter rather than separability; therefore, the optimization in [9] is not local (distributed).

power of the Tx. Moreover, $\mathbf{z} \in \mathbb{C}^{M_\mathrm{r}\times 1}$ is the additive white Gaussian noise with i.i.d. elements, i.e. $\mathbf{z} \sim \mathcal{CN}(\mathbf{0}, \sigma^2 \boldsymbol{I}_{M_\mathrm{r}})$, and $\boldsymbol{\Phi} = \mathrm{diag}\{\boldsymbol{\psi}\}$ is the phase shift matrix of the RIS elements with $\boldsymbol{\psi} = [\phi_1, ..., \phi_N]$ and $\phi_i = e^{j\varphi_i}$.

We consider spatially-correlated Rician fading model [13] for the Tx-RIS, and RIS-Rx channel statistics. Hence, the Tx-RIS channel can be modeled using a deterministic mean and a random deviation component, denoted as $\overline{\mathbf{G}} \in \mathbb{C}^{N\times M_\mathrm{t}}$ and $\widetilde{\mathbf{G}} \in \mathbb{C}^{N\times M_\mathrm{t}}$, respectively, as

$$\mathbf{G} = \sqrt{\frac{\kappa_\mathrm{G}}{\kappa_\mathrm{G}+1}}\overline{\mathbf{G}} + \sqrt{\frac{1}{\kappa_\mathrm{G}+1}}\widetilde{\mathbf{G}}, \tag{2}$$

where κ_G represents the Rician factor of the Tx-RIS channel statistic. The random component follows a circularly complex Gaussian distribution as $\mathrm{vec}(\widetilde{\mathbf{G}}) \sim \mathcal{CN}(\mathbf{0}, \mathbf{R}_\mathrm{G})$, where $\mathbf{R}_\mathrm{G} = \mathbb{E}[\mathrm{vec}(\widetilde{\mathbf{G}})\mathrm{vec}(\widetilde{\mathbf{G}})^\mathrm{H}]$ and $\mathrm{vec}(.)$ is an operator which stacks the matrix column-wise into a vector. The covariance matrix $\mathbf{R}_\mathrm{G}$ can be approximated using the Kronecker product of the RIS and Tx spatial correlation matrices as $\mathbf{R}_\mathrm{G} \approx \mathbf{R}_{\mathrm{Tx,G}} \otimes \mathbf{R}_{\mathrm{RIS,G}}$ [14], where $\mathbf{R}_{\mathrm{RIS,G}} = \frac{1}{M_\mathrm{t}}\mathbb{E}[\widetilde{\mathbf{G}}\widetilde{\mathbf{G}}^\mathrm{H}] \in \mathbb{C}^{N\times N}$ and $\mathbf{R}^*_{\mathrm{Tx,G}} = \frac{1}{N}\mathbb{E}[\widetilde{\mathbf{G}}^\mathrm{H}\widetilde{\mathbf{G}}] \in \mathbb{C}^{M_\mathrm{t}\times M_\mathrm{t}}$ are the spatial correlation matrices of the Tx-RIS channel at the Tx antennas and RIS elements, respectively. One can characterize the deviation component for the Tx-RIS channel statistic by the RIS and Tx correlation matrices [15]:

$$\widetilde{\mathbf{G}} \approx (\mathbf{R}_{\mathrm{RIS,G}})^{\frac{1}{2}}\mathbf{W}_\mathrm{G}(\mathbf{R}_{\mathrm{Tx,G}})^{\frac{1}{2}}, \tag{3}$$

where the elements of $\mathbf{W}_\mathrm{G} \in \mathbb{C}^{N\times M_\mathrm{t}}$ are independent and identically distributed random variables and follow a standard complex Gaussian distribution, i.e., $\mathrm{vec}(\mathbf{W}_\mathrm{G}) \sim \mathcal{CN}(\mathbf{0}, \mathbf{I}_{M_\mathrm{t}N})$. The RIS-Rx channel can be modeled similarly using a Rician factor κ_H as

$$\mathbf{H} = \sqrt{\frac{\kappa_\mathrm{H}}{\kappa_\mathrm{H}+1}}\overline{\mathbf{H}} + \sqrt{\frac{1}{\kappa_\mathrm{H}+1}}\widetilde{\mathbf{H}}, \tag{4}$$

where $\overline{\mathbf{H}} \in \mathbb{C}^{M_\mathrm{r}\times N}$ is the mean component of the channel statistic, which is deterministic, and $\widetilde{\mathbf{H}} \in \mathbb{C}^{M_\mathrm{r}\times N}$ is the random deviation component, which follows a circularly complex Normal distribution $\mathrm{vec}(\widetilde{\mathbf{H}}) \sim \mathcal{CN}(\mathbf{0}, \mathbf{R}_\mathrm{H})$. The random deviation component $\widetilde{\mathbf{H}}$ can be expressed similarly to (3) as

$$\widetilde{\mathbf{H}} \approx (\mathbf{R}_{\mathrm{Rx,H}})^{\frac{1}{2}}\mathbf{W}_\mathrm{H}(\mathbf{R}_{\mathrm{RIS,H}})^{\frac{1}{2}}, \tag{5}$$

where $\mathbf{W}_\mathrm{H} \in \mathbb{C}^{M_\mathrm{r}\times N}$ and $\mathrm{vec}(\mathbf{W}_\mathrm{H}) \sim \mathcal{CN}(\mathbf{0}, \mathbf{I}_{M_r N})$. Moreover, $\mathbf{R}_{\mathrm{Rx,H}} = \frac{1}{N}\mathbb{E}[\widetilde{\mathbf{H}}\widetilde{\mathbf{H}}^\mathrm{H}] \in \mathbb{C}^{M_\mathrm{r}\times M_\mathrm{r}}$ and $\mathbf{R}^*_{\mathrm{RIS,H}} = \frac{1}{M_\mathrm{r}}\mathbb{E}[\widetilde{\mathbf{H}}^\mathrm{H}\widetilde{\mathbf{H}}] \in \mathbb{C}^{N\times N}$ are the spatial correlation matrices of the RIS-Rx channel at the Rx antennas and RIS elements, respectively.

The spatial correlation matrices depend on the angles of the multipath components at the antenna arrays, the number of antennas, and antenna spacing. We assume uniform planar arrays for the Tx, Rx, and RIS antennas. Considering the planar array in the X-Y plane, we denote m as the element index in the X-axis and l as the element index in the Y-axis, starting from a fixed point. The (m, l) element of the correlation matrix at $p \in \{\mathrm{Tx}, \mathrm{Rx}, \mathrm{RIS}\}$ corresponding to the channels $\mathbf{H}$ and $\mathbf{G}$ denoted by $q \in \{\mathrm{H}, \mathrm{G}\}$, can be approximated as [16]

$$[\mathbf{R}_{p,q}]_{m,l} \approx \beta \int\int e^{j2\pi(m-l)d_{1,p}\sin(\theta)} \times e^{j2\pi(m-l)d_{2,p}\cos(\theta)\sin(\omega)} f_{p,q}(\omega, \theta) d\omega d\theta, \tag{6}$$

where β represents the total average gain of the multipath components, while $d_{1,p}$ and $d_{2,p}$ denote the vertical and horizontal antenna spacing at p, respectively. Additionally, ω and θ represent the elevation and azimuth angles of a multipath component of the channel at p with distribution $f_{p,q}$. According to the scattering model of the system, the angles ω and θ can be considered as random deviations from deterministic angles with either a Gaussian distribution or a uniform distribution. Assuming angles with a small deviation, these matrices can be further approximated as shown in [15]. With knowledge of the correlation matrices, we can design the RIS phase shifts and transmit beamforming, as further discussed in the following section.

III. Joint Transmit and RIS Beamforming Design

We aim to jointly design the beamforming vector at the transmitter and the phase shifts at the RIS to maximize the ergodic capacity. We consider the knowledge of statistical CSI at the transmitter and RIS for the beamforming design, while we assume perfect instantaneous CSI at the receiver. The ergodic capacity of this system is given by [17]

$$C = \mathbb{E}\left[\log\left(1 + \frac{\rho}{M_\mathrm{r}\sigma^2}||\mathbf{H}\boldsymbol{\Phi}\mathbf{G}\mathbf{f}||^2\right)\right]. \tag{7}$$

Using Jensen's inequality, an upper bound on the ergodic capacity is obtained as

$$C \le C_\mathrm{u} = \log(1+\gamma), \tag{8}$$

where $\gamma = \frac{\rho}{M_\mathrm{r}\sigma^2}\mathbb{E}[||\mathbf{H}\boldsymbol{\Phi}\mathbf{G}\mathbf{f}||^2]$ is the SNR. We aim to maximize the upper bound on the ergodic capacity, which leads to maximization of the SNR. Therefore, the optimization problem to design the transmit beamforming and RIS phase shifts can be written as

$$\begin{aligned} \mathrm{P1}: \max_{\mathbf{f},\boldsymbol{\psi}} \ & \mathcal{L}(\mathbf{f}, \boldsymbol{\psi}) = \mathbb{E}[||\mathbf{H}\boldsymbol{\Phi}\mathbf{G}\mathbf{f}||^2] \\ \text{s.t.} \ & ||\mathbf{f}||^2 \le 1, \\ & |\phi_i| = 1, \quad i = 1, ..., N. \end{aligned} \tag{9}$$

Due to the non-convex constraint of unit modulus phase shifts, the optimization problem P1 is non-convex. Moreover, the objective function is coupled in $\mathbf{f}$ and $\boldsymbol{\psi}$, which makes the optimization more challenging. In the following, we simplify this optimization problem to design the transmit beamforming and RIS phase shifts iteratively, when one is fixed. We obtain equivalent problems for each one, which can be solved using existing optimization approaches. Further, we simplify the equations for the Rayleigh Tx-RIS channel and show that the joint optimization problem gets decoupled.

Lemma 1 (Beamforming Vector Design)**.** *Assuming a fixed RIS phase shift vector, the beamforming vector can be obtained from the following optimization problem:*

$$\begin{aligned} \mathrm{P2}: \max_{\mathbf{f}} \ & \mathbf{f}^{\mathrm{H}}\mathbf{T}\mathbf{f} \\ \text{s.t. } & ||\mathbf{f}||^2 \leq 1, \end{aligned} \tag{10}$$

where $\mathbf{T} \in \mathbb{C}^{M_{\mathrm{t}} \times M_{\mathrm{t}}}$ *is defined as*

$$\begin{aligned} \mathbf{T} \triangleq \mathrm{unvec}\Big(& \left(\kappa_{\mathrm{G}}(\overline{\mathbf{G}}^{\mathrm{T}} \otimes \overline{\mathbf{G}}^{\mathrm{H}}) + \mathcal{R}_{\mathrm{G}}^{\mathrm{T}}\right) \\ & \times \mathrm{vec}\left((\boldsymbol{\psi}^*\boldsymbol{\psi}^{\mathrm{T}}) \odot (\kappa_{\mathrm{H}}\overline{\mathbf{H}}^{\mathrm{H}}\overline{\mathbf{H}} + \mathrm{M_r}\mathbf{R}^*_{\mathrm{RIS,H}})\right)\Big), \end{aligned} \tag{11}$$

and unvec(.) *is the reverse operator of* vec(.) *and* $\otimes$ *and* $\odot$ *are the Kronecker and Hadamard products, respectively.*

Proof. The proof is provided in Appendix A. □

The optimization problem P2 is quadratic with an L_2 norm constraint and is a convex optimization. Since $\mathbf{T}$ is a positive semidefinite matrix, by employing the eigenvalue decomposition of $\mathbf{T}$ and representing $\mathbf{f}$ as a linear combination of the orthogonal eigenvectors of $\mathbf{T}$, it can be readily shown that its optimal solution is $\mathbf{f} = \mathbf{u}$, where $\mathbf{u} = [u_1, \ldots, u_N]^{\mathrm{T}}$ represents the dominant eigenvector (the eigenvector corresponding to the dominant eigenvalue) of $\mathbf{T}$. As can be observed, the beamforming design depends on the mean components of the Tx-RIS and RIS-Rx channels, i.e., $\overline{\mathbf{G}}$ and $\overline{\mathbf{H}}$, as well as the spatial correlation matrices $\mathbf{R}_{\mathrm{Tx,G}}$, $\mathbf{R}_{\mathrm{RIS,G}}$, and $\mathbf{R}_{\mathrm{RIS,H}}$, and it is independent of the spatial correlation matrix at the Rx antennas. Knowing the spatial correlation matrices of the channels at the RIS and Tx sides, one can calculate the matrix $\mathbf{Q}$ and choose the phase shift vector $\boldsymbol{\psi}$ through the above optimization problem.

Lemma 2 (RIS Phase Shift Design)**.** *Assuming a fixed beamforming vector, the optimization problem for designing RIS phase shifts is*

$$\begin{aligned} \mathrm{P3}: \max_{\boldsymbol{\psi}} \ & \boldsymbol{\psi}^{\mathrm{H}}\mathbf{Q}\boldsymbol{\psi} \\ \text{s.t. } & |\phi_i| = 1, \quad i = 1, ..., N, \end{aligned} \tag{12}$$

where $\mathbf{Q} \in \mathbb{C}^{N \times N}$ *is defined as*

$$\begin{aligned} \mathbf{Q} \triangleq \mathrm{unvec}\Big(& \left(\kappa_{\mathrm{G}}(\overline{\mathbf{G}} \otimes \overline{\mathbf{G}}^*) + \mathcal{R}_{\mathrm{G}}\right)\mathrm{vec}(\mathbf{f}^*\mathbf{f}^{\mathrm{T}})\Big) \\ & \odot \left(\kappa_{\mathrm{H}}\overline{\mathbf{H}}^{\mathrm{H}}\overline{\mathbf{H}} + M_{\mathrm{r}}\mathbf{R}^*_{\mathrm{RIS,H}}\right). \end{aligned} \tag{13}$$

Proof. The proof is provided in Appendix B. □

Similar to the beamforming vector design problem, obtaining the RIS phase shifts requires the mean components of the channels, the correlation matrix of the Tx-RIS channel at the Tx antennas, and the correlation matrices of the Tx-RIS and RIS-Rx channels at the RIS elements. However, in contrast to the beamforming vector design problem, this optimization problem is non-convex due to the non-convex constraint and is generally an NP-hard problem [18]. Several approaches exist to address this non-convex optimization problem, such as semidefinite program (SDP) relaxation [18] and convex relaxation [15].

In the convex relaxation method presented in [15], the unit-modulus constraint in the optimization problem P3 is replaced with an L_2 norm constraint. We then seek the solution to the following optimization problem:

$$\begin{aligned} \mathrm{P4}: \max_{\boldsymbol{\psi}} \ & \boldsymbol{\psi}^{\mathrm{H}}\mathbf{Q}\boldsymbol{\psi} \\ \text{s.t. } & ||\boldsymbol{\psi}||^2 \leq N. \end{aligned} \tag{14}$$

The optimization problem P4 is convex and the optimum phase shift vector can be obtained similar to (14) as $\boldsymbol{\psi} = \sqrt{N}\mathbf{v}$, where $\mathbf{v} = [v_1, \ldots, v_N]^{\mathrm{T}}$ represents the dominant eigenvector of $\mathbf{Q}$. Therefore, to obtain the solution of P3, we can choose $\boldsymbol{\psi}$ in the direction of $\mathbf{v}$. More specifically, each element of the RIS phase shift vector is chosen as $\hat{\psi}_i = e^{j \arg\{v_i\}}$ [15].

In the SDP relaxation approach, the optimization problem P3 is reformulated as [18]

$$\begin{aligned} \mathrm{P5}: \max_{\boldsymbol{\Phi}} \ & \mathrm{tr}\{\mathbf{Q}\boldsymbol{\Phi}\} \\ \text{s.t. } & [\boldsymbol{\Phi}]_{ii} = 1, \quad i = 1, ..., N, \\ & \boldsymbol{\Phi} \geq 0, \ \mathrm{Rank}(\boldsymbol{\Phi}) = 1. \end{aligned} \tag{15}$$

By relaxing the rank-1 constraint, the optimization problem is transformed into a convex SDP that can be solved using convex optimization solvers such as CVX. Subsequently, an approximate solution to the original optimization problem can be derived based on this solution as follows [19]:

1. Let $\hat{\boldsymbol{\Phi}}$ be the solution for SDP relaxation. Apply Cholesky decomposition on $\hat{\boldsymbol{\Phi}}$, yielding $\hat{\boldsymbol{\Phi}} = \mathbf{K}\mathbf{K}^{\mathrm{H}}$.
2. Generate a circularly Gaussian random vector $\mathbf{r} \in \mathcal{CN}(\mathbf{0}, \mathbf{I}_{\mathrm{N}})$.
3. Let the approximate solution for (12) be $\hat{\phi}_i = e^{j \arg(s_i)}$, $i = 1, ..., N$, where $[s_1, ..., s_N]^{\mathrm{T}} = \mathbf{K}\mathbf{r}$.

Lemma 3 (Separability of Beamforming and RIS Design)**.** *When the Tx-RIS channel follows a Rayleigh fading model, i.e.,* $\kappa_{\mathrm{G}} = 0$*, the joint optimization problem* P1 *in* (9) *for* $\mathbf{f}$ *and* $\boldsymbol{\psi}$ *can be decoupled into two disjoint problems:*
1) Optimizing Tx beamforming vector $\mathbf{f}$*:*

$$\begin{aligned} \mathrm{P6}: \max_{\mathbf{f}} \ & \mathbf{f}^{\mathrm{H}}\mathbf{R}_{\mathrm{Tx,G}}\mathbf{f} \\ \text{s.t. } & ||\mathbf{f}||^2 \leq 1. \end{aligned} \tag{16}$$

2) Optimizing RIS phase shift vector $\boldsymbol{\psi}$*:*

$$\begin{aligned} \mathrm{P7}: \max_{\boldsymbol{\psi}} \ & \boldsymbol{\psi}^{\mathrm{H}}\left(\mathbf{R}^*_{\mathrm{RIS,G}} \odot (\kappa_{\mathrm{H}}\overline{\mathbf{H}}^{\mathrm{H}}\overline{\mathbf{H}} + M_{\mathrm{r}}\mathbf{R}^*_{\mathrm{RIS,H}})\right)\boldsymbol{\psi} \\ \text{s.t. } & |\phi_i| = 1, \quad i = 1, ..., N. \end{aligned} \tag{17}$$

Proof. The proof is provided in Appendix C. □

It is worth mentioning that the decoupling of the two optimization problems is solely due to the Rayleigh Tx-RIS channel and is valid for both Rayleigh and Rician RIS-Rx channels. As a result, for the Rayleigh Tx-RIS channel, in the absence of channel estimates and relying solely on the long-term channel statistics, the transmit beamforming and RIS phase shift vectors are designed independently. The transmit

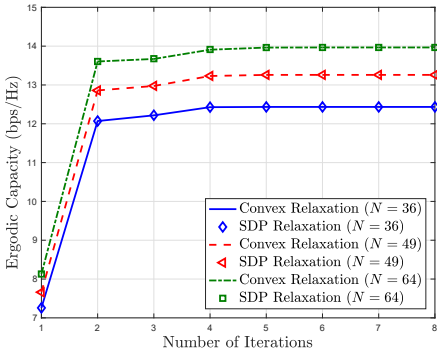

Fig. 1. Ergodic capacity versus the number of iterations for Rician channels.

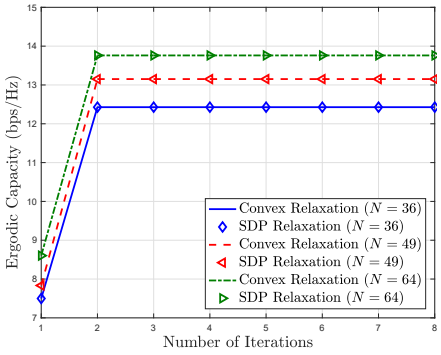

Fig. 2. Ergodic capacity versus the number of iterations for the Rayleigh Tx-RIS channel.

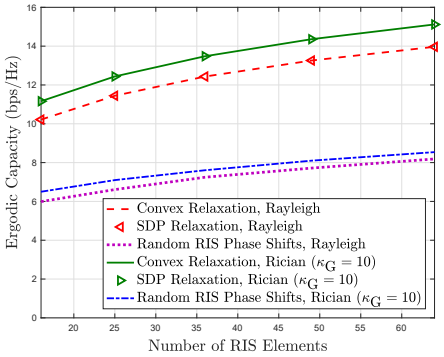

Fig. 3. Ergodic capacity versus the number of RIS elements.

beamforming is designed based on the spatial correlation matrix at the transmitter and the RIS phase shifts are designed utilizing RIS correlation matrices.

IV. Numerical Results

In this section, we present the numerical results to verify our findings in designing RIS phase shifts and Tx beamforming vectors in two cases of Rayleigh and Rician Tx-RIS channels. We consider a MIMO system with 10 transmit and receive antennas. To construct the mean components and correlation matrices of the channel statistics, we randomly generate elevation and azimuth angles from uniform distributions within the ranges $[0, \pi]$ and $[0, 2\pi]$, respectively.

Specifically, we utilize the approximated expression presented in [16] to obtain the correlation matrices and the expression presented in [20] for the mean components. Throughout the simulations, we assume $\frac{\rho}{\sigma^2}$ to be 10 dB and the upper bound on the ergodic capacity is calculated according to (8) using the simplified equations for SNR in (27) and (22). The antenna spacing for Tx, Rx, and RIS are $d_{\mathrm{Tx}} = d_{\mathrm{Rx}} = \frac{\lambda}{2}$ and $d_{\mathrm{RIS}} = \frac{\lambda}{4}$, respectively, where λ is the carrier wavelength associated with the carrier frequency of 0.3 GHz.

In Fig. 1, we depict the upper bound on the ergodic capacity against the number of iterations required to achieve the optimal designs for different numbers of RIS elements, assuming the channels to be Rician with $\kappa_{\mathrm{G}} = \kappa_{\mathrm{H}} = 1$. In the first iteration, the RIS phase shift vector is set as a random vector. In the next iteration, the beamforming vector is designed based on the optimal solution for the optimization problem P3 using the random RIS phase shift. Then, the RIS beamforming is designed using the suboptimal solution for P5 in the convex relaxation case and the suboptimal solution for P6 in the SDP relaxation. This process continues iteratively until the rate converges. It can be seen that both the convex and SDP relaxations result in the same answer, and the optimal designs are obtained after a few steps.

The same setting is utilized in Fig. 2 for the case where the Tx-RIS channel is Rayleigh, i.e., $\kappa_{\mathrm{G}} = 0$, while the RIS-Rx channel is Rician with $\kappa_{\mathrm{G}} = 1$. In this case, the presented iterative algorithm converges after the first step. This is due to the fact that for the Rayleigh Tx-RIS channel, the optimization problems are decoupled, as mentioned previously. Hence, the optimal passive and active beamformings can be obtained in one iteration using the solutions for P8 and P9, respectively, and there is no need to use the iterative algorithm.

To observe the effect of the number of RIS elements on the optimal design under Rician and Rayleigh assumptions, the corresponding upper bounds on the ergodic capacity are provided in Fig. 3. For the Rayleigh case, we have $\kappa_{\mathrm{G}} = 0$, and for the Rician case, we assume $\kappa_{\mathrm{G}} = 10$. In both cases, we assume $\kappa_{\mathrm{H}} = 10$. It can be seen from the figure that as the number of RIS elements increases, the rate is improved for both Rician and Rayleigh channels. The optimal Tx beamforming and suboptimal RIS phase shifts result in a higher rate in the Rician channels compared to the Rayleigh channel, due to employing the mean components and jointly designing the passive and active beamforming. The results are compared with the case where RIS is adjusted randomly and the beamforming vector is designed based on P8, which demonstrates the effectiveness of the proposed beamforming designs.

V. Conclusion

In this paper, we investigated the design of RIS phase shifts and transmit beamforming in a correlated Rician fading RIS-aided MIMO channel to improve the ergodic capacity while utilizing only channel statistics. Employing an iterative algorithm, we optimally designed the transmit beamforming and sub-optimally designed the RIS phase shifts. Additionally, we studied the special case of the correlated Rayleigh model, which results in the optimization problem being simplified to two disjoint design problems for RIS phase shifts and transmit beamforming. Using numerical results, we showed that the proposed iterative algorithm converges in a few iterations for the general Rician channels. For the Rayleigh channel, it converges in a single iteration, which validates our result on the design problems being disjoint.

APPENDIX A

We assume a fixed RIS phase shift vector and obtain the beamforming vector from the following optimization problem:

$$\begin{aligned} \text{P8}: \max_{\mathbf{f}} \;& \mathcal{L}(\mathbf{f},\boldsymbol{\psi}) = \mathbb{E}[||\mathbf{H}\boldsymbol{\Phi}\mathbf{G}\mathbf{f}||^2] \\ \text{s.t. } & ||\mathbf{f}||^2 \le 1. \end{aligned} \tag{18}$$

The objective function $\mathcal{L}(\mathbf{f},\boldsymbol{\psi})$ can be simplified as follows:

$$\begin{aligned} \mathcal{L}(\mathbf{f},\boldsymbol{\psi}) &= \mathbb{E}\big[\mathbf{f}^{\mathrm{H}}\mathbf{G}^{\mathrm{H}}\boldsymbol{\Phi}^{\mathrm{H}}\mathbf{H}^{\mathrm{H}}\mathbf{H}\boldsymbol{\Phi}\mathbf{G}\mathbf{f}\big] \\ &= \mathbf{f}^{\mathrm{H}}\mathbb{E}\big[\mathbf{G}^{\mathrm{H}}\boldsymbol{\Phi}^{\mathrm{H}}\mathbb{E}[\mathbf{H}^{\mathrm{H}}\mathbf{H}|\mathbf{G}]\boldsymbol{\Phi}\mathbf{G}\big]\mathbf{f} \\ &= \mathbf{f}^{\mathrm{H}}\mathrm{unvec}\left(\mathbb{E}\left[\left((\boldsymbol{\Phi}\mathbf{G})^{\mathrm{T}}\otimes(\boldsymbol{\Phi}\mathbf{G})^{\mathrm{H}}\right)\mathrm{vec}(\mathbb{E}[\mathbf{H}^{\mathrm{H}}\mathbf{H}])\right]\right)\mathbf{f} \\ &= \mathbf{f}^{\mathrm{H}}\mathrm{unvec}\left(\mathbb{E}\left[(\boldsymbol{\Phi}\mathbf{G})^{\mathrm{T}}\otimes(\boldsymbol{\Phi}\mathbf{G})^{\mathrm{H}}\right]\mathrm{vec}(\mathbb{E}[\mathbf{H}^{\mathrm{H}}\mathbf{H}])\right)\mathbf{f} \\ &= \mathbf{f}^{\mathrm{H}}\mathrm{unvec}\left(\mathbb{E}[\mathbf{G}^{\mathrm{T}}\otimes\mathbf{G}^{\mathrm{H}}](\boldsymbol{\Phi}^{\mathrm{T}}\otimes\boldsymbol{\Phi}^{\mathrm{H}})\mathrm{vec}(\mathbb{E}[\mathbf{H}^{\mathrm{H}}\mathbf{H}])\right)\mathbf{f}, \end{aligned} \tag{19}$$

The equalities are derived using the law of total expectations and the properties of the Kronecker product. It can be easily seen that $\boldsymbol{\Phi}^{\mathrm{T}}\otimes\boldsymbol{\Phi}^{\mathrm{H}} = \mathrm{diag}(\mathrm{vec}(\boldsymbol{\psi}^{*}\boldsymbol{\psi}^{\mathrm{T}}))$. Hence,

$$\begin{aligned} &\mathcal{L}(\mathbf{f},\boldsymbol{\psi}) \\ &= \mathbf{f}^{\mathrm{H}}\mathrm{unvec}\left(\mathbb{E}[\mathbf{G}^{\mathrm{T}}\otimes\mathbf{G}^{\mathrm{H}}]\mathrm{diag}(\mathrm{vec}(\boldsymbol{\psi}^{*}\boldsymbol{\psi}^{\mathrm{T}}))\mathrm{vec}(\mathbb{E}[\mathbf{H}^{\mathrm{H}}\mathbf{H}])\right)\mathbf{f} \\ &= \mathbf{f}^{\mathrm{H}}\mathrm{unvec}\left(\mathbb{E}[\mathbf{G}\otimes\mathbf{G}^{*}]^{\mathrm{T}}\big(\mathrm{vec}(\boldsymbol{\psi}^{*}\boldsymbol{\psi}^{\mathrm{T}})\odot\mathrm{vec}(\mathbb{E}[\mathbf{H}^{\mathrm{H}}\mathbf{H}])\big)\right)\mathbf{f} \\ &= \mathbf{f}^{\mathrm{H}}\mathrm{unvec}\left(\mathbb{E}[\mathbf{G}\otimes\mathbf{G}^{*}]^{\mathrm{T}}\mathrm{vec}\big((\boldsymbol{\psi}^{*}\boldsymbol{\psi}^{\mathrm{T}})\odot\mathbb{E}[\mathbf{H}^{\mathrm{H}}\mathbf{H}]\big)\right)\mathbf{f}. \end{aligned} \tag{20}$$

Using (2) and (4), we have

$$\begin{aligned} \mathbb{E}[\mathbf{G}\otimes\mathbf{G}^{*}] &= \frac{\kappa_{\mathrm{G}}}{\kappa_{\mathrm{G}}+1}(\overline{\mathbf{G}}\otimes\overline{\mathbf{G}}^{*}) + \frac{1}{\kappa_{\mathrm{G}}+1}\mathbb{E}[\widetilde{\mathbf{G}}\otimes\widetilde{\mathbf{G}}^{*}] \\ \mathbb{E}[\mathbf{H}^{\mathrm{H}}\mathbf{H}] &= \frac{\kappa_{\mathrm{H}}}{\kappa_{\mathrm{H}}+1}\overline{\mathbf{H}}^{\mathrm{H}}\overline{\mathbf{H}} + \frac{M_{\mathrm{r}}}{\kappa_{\mathrm{H}}+1}\mathbf{R}^{*}_{\mathrm{RIS,H}}. \end{aligned} \tag{21}$$

We define $\mathcal{R}_{\mathrm{G}} \triangleq \mathbb{E}[\widetilde{\mathbf{G}}\otimes\widetilde{\mathbf{G}}^{*}]$, which can be approximated using (3) by $\mathcal{R}_{\mathrm{G}} \approx \mathrm{vec}(\mathbf{R}^{*}_{\mathrm{RIS,G}})\left(\mathrm{vec}(\mathbf{R}_{\mathrm{Tx,G}})\right)^{\mathrm{T}}$ (the derivation is omitted for brevity). Hence, $\mathcal{L}(\mathbf{f},\boldsymbol{\psi})$ can be obtained as

$$\begin{aligned} \mathcal{L}(\mathbf{f},\boldsymbol{\psi}) = \mathbf{f}^{\mathrm{H}}\mathrm{unvec}\Bigg(&\Big(\frac{\kappa_{\mathrm{G}}}{\kappa_{\mathrm{G}}+1}(\overline{\mathbf{G}}^{\mathrm{T}}\otimes\overline{\mathbf{G}}^{\mathrm{H}}) + \frac{1}{\kappa_{\mathrm{G}}+1}\mathcal{R}_{\mathrm{G}}^{\mathrm{T}}\Big) \\ &\times\mathrm{vec}\big((\boldsymbol{\psi}^{*}\boldsymbol{\psi}^{\mathrm{T}})\odot\big(\frac{\kappa_{\mathrm{H}}}{\kappa_{\mathrm{H}}+1}\overline{\mathbf{H}}^{\mathrm{H}}\overline{\mathbf{H}} + \frac{M_{\mathrm{r}}}{\kappa_{\mathrm{H}}+1}\mathbf{R}^{*}_{\mathrm{RIS,H}}\big)\big)\Bigg)\mathbf{f}. \end{aligned} \tag{22}$$

APPENDIX B

We design the RIS phase shift vector $\boldsymbol{\psi}$ assuming a fixed beamforming vector $\mathbf{f}$ using the following optimization problem:

$$\begin{aligned} \text{P9}: \max_{\boldsymbol{\psi}} \;& \mathcal{L}(\mathbf{f},\boldsymbol{\psi}) = \mathbb{E}[||\mathbf{H}\boldsymbol{\Phi}\mathbf{G}\mathbf{f}||^2] \\ \text{s.t. } & |\phi_i| = 1, \quad i = 1,...,N. \end{aligned} \tag{23}$$

We simplify the objective function $\mathcal{L}(\mathbf{f},\boldsymbol{\psi})$ using Kronecker product properties as

$$\begin{aligned} \mathcal{L}(\mathbf{f},\boldsymbol{\psi}) &= \mathbb{E}[\mathbf{f}^{\mathrm{H}}\mathbf{G}^{\mathrm{H}}\boldsymbol{\Phi}^{\mathrm{H}}\mathbf{H}^{\mathrm{H}}\mathbf{H}\boldsymbol{\Phi}\mathbf{G}\mathbf{f}] \\ &= \mathbb{E}\big[\mathbf{f}^{\mathrm{H}}\mathbf{G}^{\mathrm{H}}\boldsymbol{\Phi}^{\mathrm{H}}\mathbb{E}[\mathbf{H}^{\mathrm{H}}\mathbf{H}|\mathbf{G}]\boldsymbol{\Phi}\mathbf{G}\mathbf{f}\big] \\ &= \mathbb{E}\big[\big((\boldsymbol{\Phi}\mathbf{G}\mathbf{f})^{\mathrm{T}}\otimes(\boldsymbol{\Phi}\mathbf{G}\mathbf{f})^{\mathrm{H}}\big)\mathrm{vec}(\mathbb{E}[\mathbf{H}^{\mathrm{H}}\mathbf{H}])\big] \\ &= \mathbb{E}\big[(\boldsymbol{\Phi}\mathbf{G}\mathbf{f})^{\mathrm{T}}\otimes(\boldsymbol{\Phi}\mathbf{G}\mathbf{f})^{\mathrm{H}}\big]\mathrm{vec}(\mathbb{E}[\mathbf{H}^{\mathrm{H}}\mathbf{H}]) \\ &= \mathbb{E}\big[(\mathbf{G}\mathbf{f})^{\mathrm{T}}\otimes(\mathbf{G}\mathbf{f})^{\mathrm{H}}\big](\boldsymbol{\Phi}^{\mathrm{T}}\otimes\boldsymbol{\Phi}^{\mathrm{H}})\mathrm{vec}(\mathbb{E}[\mathbf{H}^{\mathrm{H}}\mathbf{H}]) \\ &= \mathbb{E}\big[\mathrm{vec}((\mathbf{G}\mathbf{f})^{*}(\mathbf{G}\mathbf{f})^{\mathrm{T}})\big]^{\mathrm{T}}(\boldsymbol{\Phi}^{\mathrm{T}}\otimes\boldsymbol{\Phi}^{\mathrm{H}})\mathrm{vec}(\mathbb{E}[\mathbf{H}^{\mathrm{H}}\mathbf{H}]). \end{aligned} \tag{24}$$

$\mathcal{L}(\mathbf{f},\boldsymbol{\psi})$ can be further simplified using $\boldsymbol{\Phi}^{\mathrm{T}}\otimes\boldsymbol{\Phi}^{\mathrm{H}} = \mathrm{diag}(\mathrm{vec}(\boldsymbol{\psi}^{*}\boldsymbol{\psi}^{\mathrm{T}}))$ as follows:

$$\begin{aligned} &\mathcal{L}(\mathbf{f},\boldsymbol{\psi}) \\ &= \mathbb{E}\big[\mathrm{vec}((\mathbf{G}\mathbf{f})^{*}(\mathbf{G}\mathbf{f})^{\mathrm{T}})\big]^{\mathrm{T}}\mathrm{diag}(\mathrm{vec}(\boldsymbol{\psi}^{*}\boldsymbol{\psi}^{\mathrm{T}}))\mathrm{vec}(\mathbb{E}[\mathbf{H}^{\mathrm{H}}\mathbf{H}]) \\ &= \big(\mathrm{vec}(\mathbb{E}\big[\mathbf{G}^{*}(\mathbf{f}^{*}\mathbf{f}^{\mathrm{T}})\mathbf{G}^{\mathrm{T}}\big])\big)^{\mathrm{T}}\mathrm{diag}(\mathrm{vec}(\mathbb{E}[\mathbf{H}^{\mathrm{H}}\mathbf{H}]))\mathrm{vec}(\boldsymbol{\psi}^{*}\boldsymbol{\psi}^{\mathrm{T}}) \\ &= \big(\mathrm{vec}(\mathbb{E}\big[\mathbf{G}^{*}(\mathbf{f}^{*}\mathbf{f}^{\mathrm{T}})\mathbf{G}^{\mathrm{T}}\big]\odot\mathbb{E}[\mathbf{H}^{\mathrm{H}}\mathbf{H}])\big)^{\mathrm{T}}\mathrm{vec}(\boldsymbol{\psi}^{*}\boldsymbol{\psi}^{\mathrm{T}}). \end{aligned} \tag{25}$$

It can be easily shown that for a matrix $\mathbf{A}$ and a vector $\mathbf{a}$, we have $(\mathrm{vec}(\mathbf{A}))^{\mathrm{T}}\mathrm{vec}(\mathbf{a}^{*}\mathbf{a}) = \mathbf{a}^{\mathrm{H}}\mathbf{A}\mathbf{a}$. Hence,

$$\begin{aligned} \mathcal{L}(\mathbf{f},\boldsymbol{\psi}) &= \boldsymbol{\psi}^{\mathrm{H}}\big(\mathbb{E}\big[\mathbf{G}^{*}(\mathbf{f}^{*}\mathbf{f}^{\mathrm{T}})\mathbf{G}^{\mathrm{T}}\big]\odot\mathbb{E}[\mathbf{H}^{\mathrm{H}}\mathbf{H}]\big)\boldsymbol{\psi} \\ &= \boldsymbol{\psi}^{\mathrm{H}}\big(\mathbb{E}\big[\mathrm{unvec}((\mathbf{G}\otimes\mathbf{G}^{*})\mathrm{vec}(\mathbf{f}^{*}\mathbf{f}^{\mathrm{T}}))\big]\odot\mathbb{E}[\mathbf{H}^{\mathrm{H}}\mathbf{H}]\big)\boldsymbol{\psi} \\ &= \boldsymbol{\psi}^{\mathrm{H}}\big(\mathrm{unvec}\big(\mathbb{E}\big[\mathbf{G}\otimes\mathbf{G}^{*}\big]\mathrm{vec}(\mathbf{f}^{*}\mathbf{f}^{\mathrm{T}})\big)\odot\mathbb{E}[\mathbf{H}^{\mathrm{H}}\mathbf{H}]\big)\boldsymbol{\psi}. \end{aligned} \tag{26}$$

Now, using (21), we have

$$\begin{aligned} \mathcal{L}(\mathbf{f},\boldsymbol{\psi}) = \boldsymbol{\psi}^{\mathrm{H}}\Bigg(&\mathrm{unvec}\big(\big(\frac{\kappa_{\mathrm{G}}}{\kappa_{\mathrm{G}}+1}(\overline{\mathbf{G}}\otimes\overline{\mathbf{G}}^{*}) + \frac{1}{\kappa_{\mathrm{G}}+1}\mathcal{R}_{\mathrm{G}}\big) \\ &\times\mathrm{vec}(\mathbf{f}^{*}\mathbf{f}^{\mathrm{T}})\big)\odot\big(\frac{\kappa_{\mathrm{H}}}{\kappa_{\mathrm{H}}+1}\overline{\mathbf{H}}^{\mathrm{H}}\overline{\mathbf{H}} + \frac{M_{\mathrm{r}}}{\kappa_{\mathrm{H}}+1}\mathbf{R}^{*}_{\mathrm{RIS,H}}\big)\Bigg)\boldsymbol{\psi}. \end{aligned} \tag{27}$$

APPENDIX C

For the Rayleigh Tx-RIS channel, i.e., $\kappa_{\mathrm{G}} = 0$, the objective function $\mathcal{L}(\mathbf{f},\boldsymbol{\psi})$ can be simplified according to (22) as follows:

$$\begin{aligned} \mathcal{L}(\mathbf{f},\boldsymbol{\psi}) = \mathbf{f}^{\mathrm{H}}\mathrm{unvec}\Bigg(&\mathrm{vec}(\mathbf{R}_{\mathrm{Tx,G}})\left(\mathrm{vec}(\mathbf{R}^{*}_{\mathrm{RIS,G}})\right)^{\mathrm{T}} \\ &\times\mathrm{vec}\big((\boldsymbol{\psi}^{*}\boldsymbol{\psi}^{\mathrm{T}})\odot\big(\frac{\kappa_{\mathrm{H}}}{\kappa_{\mathrm{H}}+1}\overline{\mathbf{H}}^{\mathrm{H}}\overline{\mathbf{H}} + \frac{M_{\mathrm{r}}}{\kappa_{\mathrm{H}}+1}\mathbf{R}^{*}_{\mathrm{RIS,H}}\big)\big)\Bigg)\mathbf{f}. \end{aligned} \tag{28}$$

Now, since $\left(\mathrm{vec}(\mathbf{R}^{*}_{\mathrm{RIS,G}})\right)^{\mathrm{T}}\mathrm{vec}\big((\boldsymbol{\psi}^{*}\boldsymbol{\psi}^{\mathrm{T}})\odot(\frac{\kappa_{\mathrm{H}}}{\kappa_{\mathrm{H}}+1}\overline{\mathbf{H}}^{\mathrm{H}}\overline{\mathbf{H}} + \frac{M_{\mathrm{r}}}{\kappa_{\mathrm{H}}+1}\mathbf{R}^{*}_{\mathrm{RIS,H}})\big)$ is a scalar, it can come out of the unvec operation. Hence, we have

$$\begin{aligned} \mathcal{L}(\mathbf{f},\boldsymbol{\psi}) &= \Bigg(\mathbf{f}^{\mathrm{H}}\mathrm{unvec}\big(\mathrm{vec}(\mathbf{R}_{\mathrm{Tx,G}})\big)\mathbf{f}\Bigg)\Bigg(\left(\mathrm{vec}(\mathbf{R}^{*}_{\mathrm{RIS,G}})\right)^{\mathrm{T}} \\ &\quad\times\mathrm{vec}\big((\boldsymbol{\psi}^{*}\boldsymbol{\psi}^{\mathrm{T}})\odot\big(\frac{\kappa_{\mathrm{H}}}{\kappa_{\mathrm{H}}+1}\overline{\mathbf{H}}^{\mathrm{H}}\overline{\mathbf{H}} + \frac{M_{\mathrm{r}}}{\kappa_{\mathrm{H}}+1}\mathbf{R}^{*}_{\mathrm{RIS,H}}\big)\big)\Bigg) \\ &= \Bigg(\mathbf{f}^{\mathrm{H}}\mathbf{R}_{\mathrm{Tx,G}}\mathbf{f}\Bigg)\Bigg(\big(\mathrm{vec}(\mathbf{R}^{*}_{\mathrm{RIS,G}}\odot\big(\frac{\kappa_{\mathrm{H}}}{\kappa_{\mathrm{H}}+1}\overline{\mathbf{H}}^{\mathrm{H}}\overline{\mathbf{H}} \\ &\quad+\frac{M_{\mathrm{r}}}{\kappa_{\mathrm{H}}+1}\mathbf{R}^{*}_{\mathrm{RIS,H}}\big)\big)^{\mathrm{T}}\mathrm{vec}\big((\boldsymbol{\psi}^{*}\boldsymbol{\psi}^{\mathrm{T}})\big)\Bigg) \\ &= \Bigg(\mathbf{f}^{\mathrm{H}}\mathbf{R}_{\mathrm{Tx,G}}\mathbf{f}\Bigg)\Bigg(\boldsymbol{\psi}^{\mathrm{H}}\big(\mathbf{R}^{*}_{\mathrm{RIS,G}}\odot\big(\frac{\kappa_{\mathrm{H}}}{\kappa_{\mathrm{H}}+1}\overline{\mathbf{H}}^{\mathrm{H}}\overline{\mathbf{H}} \\ &\quad+\frac{M_{\mathrm{r}}}{\kappa_{\mathrm{H}}+1}\mathbf{R}^{*}_{\mathrm{RIS,H}}\big)\big)\boldsymbol{\psi}\Bigg). \end{aligned} \tag{29}$$

This could also be achieved by setting κ_{G} to 0 in (27). Now, since $\mathbf{f}^{\mathrm{H}}\mathbf{R}_{\mathrm{Tx,G}}\mathbf{f}$ is a scalar independent of $\boldsymbol{\psi}$, and $\boldsymbol{\psi}^{\mathrm{H}}\big(\mathbf{R}^{*}_{\mathrm{RIS,G}}\odot(\frac{\kappa_{\mathrm{H}}}{\kappa_{\mathrm{H}}+1}\overline{\mathbf{H}}^{\mathrm{H}}\overline{\mathbf{H}} + \frac{M_{\mathrm{r}}}{\kappa_{\mathrm{H}}+1}\mathbf{R}^{*}_{\mathrm{RIS,H}})\big)\boldsymbol{\psi}$ is a scalar independent of $\mathbf{f}$, the joint optimization problem P1 in (9) for $\mathbf{f}$ and $\boldsymbol{\psi}$ can be decoupled into two disjoint problems of P6 and P7.

REFERENCES

[1] M. Di Renzo, A. Zappone, M. Debbah, M.-S. Alouini, C. Yuen, J. de Rosny, and S. Tretyakov, "Smart radio environments empowered by reconfigurable intelligent surfaces: How it works, state of research, and the road ahead," *IEEE Journal on Selected Areas in Communications*, vol. 38, no. 11, pp. 2450–2525, 2020.

[2] C. Pan, H. Ren, K. Wang, W. Xu, M. Elkashlan, A. Nallanathan, and L. Hanzo, "Multicell MIMO communications relying on intelligent reflecting surfaces," *IEEE Transactions on Wireless Communications*, vol. 19, no. 8, pp. 5218–5233, 2020.

[3] W. Yan, X. Yuan, Z.-Q. He, and X. Kuai, "Passive beamforming and information transfer design for reconfigurable intelligent surfaces aided multiuser MIMO systems," *IEEE Journal on Selected Areas in Communications*, vol. 38, no. 8, pp. 1793–1808, 2020.

[4] B. Shamasundar, N. Daryanavardan, and A. Nosratinia, "Channel training & estimation for reconfigurable intelligent surfaces: Exposition of principles, approaches, and open problems," *IEEE Access*, vol. 11, pp. 6717–6734, 2023.

[5] B. Shamasundar and A. Nosratinia, "Canonical training is bad for reconfigurable intelligent surfaces," in *2022 IEEE International Symposium on Information Theory (ISIT)*. IEEE, 2022, pp. 2499–2504.

[6] X. Gan, C. Zhong, C. Huang, and Z. Zhang, "RIS-assisted multi-user MISO communications exploiting statistical CSI," *IEEE Transactions on Communications*, vol. 69, no. 10, pp. 6781–6792, 2021.

[7] J. Wang, H. Wang, Y. Han, S. Jin, and X. Li, "Joint transmit beamforming and phase shift design for reconfigurable intelligent surface assisted MIMO systems," *IEEE Transactions on Cognitive Communications and Networking*, vol. 7, no. 2, pp. 354–368, 2021.

[8] K. Xu, J. Zhang, X. Yang, S. Ma, and G. Yang, "On the sum-rate of RIS-assisted MIMO multiple-access channels over spatially correlated rician fading," *IEEE Transactions on Communications*, vol. 69, no. 12, pp. 8228–8241, 2021.

[9] H. Zhang, S. Ma, Z. Shi, X. Zhao, and G. Yang, "Sum-rate maximization of RIS-aided multi-user MIMO systems with statistical CSI," *IEEE Transactions on Wireless Communications*, vol. 22, no. 7, pp. 4788–4801, 2023.

[10] Z. Yu, Y. Han, M. Matthaiou, X. Li, and S. Jin, "Statistical CSI-based design for RIS-assisted communication systems," *IEEE Wireless Communications Letters*, vol. 11, no. 10, pp. 2115–2119, 2022.

[11] Y. Han, W. Tang, S. Jin, C.-K. Wen, and X. Ma, "Large intelligent surface-assisted wireless communication exploiting statistical CSI," *IEEE Transactions on Vehicular Technology*, vol. 68, no. 8, pp. 8238–8242, 2019.

[12] M.-M. Zhao, Q. Wu, M.-J. Zhao, and R. Zhang, "Intelligent reflecting surface enhanced wireless networks: Two-timescale beamforming optimization," *IEEE Transactions on Wireless Communications*, vol. 20, no. 1, pp. 2–17, 2021.

[13] Ö. T. Demir and E. Björnson, "Large-scale fading precoding for maximizing the product of SINRs," in *ICASSP 2020-2020 IEEE International Conference on Acoustics, Speech and Signal Processing (ICASSP)*. IEEE, 2020, pp. 5150–5154.

[14] N. Shariati and M. Bengtsson, "How far from Kronecker can a MIMO channel be? Does it matter?" in *17th European Wireless 2011-Sustainable Wireless Technologies*. VDE, 2011, pp. 1–7.

[15] Ö. T. Demir and E. Björnson, "Is channel estimation necessary to select phase-shifts for RIS-assisted massive MIMO?" *IEEE Transactions on Wireless Communications*, vol. 21, no. 11, pp. 9537–9552, 2022.

[16] E. Björnson, J. Hoydis, L. Sanguinetti *et al.*, "Massive MIMO networks: Spectral, energy, and hardware efficiency," *Foundations and Trends® in Signal Processing*, vol. 11, no. 3-4, pp. 154–655, 2017.

[17] A. Goldsmith, S. A. Jafar, N. Jindal, and S. Vishwanath, "Capacity limits of MIMO channels," *IEEE Journal on selected areas in Communications*, vol. 21, no. 5, pp. 684–702, 2003.

[18] Q. Wu and R. Zhang, "Intelligent reflecting surface enhanced wireless network: Joint active and passive beamforming design," in *2018 IEEE Global Communications Conference (GLOBECOM)*. IEEE, 2018, pp. 1–6.

[19] A. M.-C. So, J. Zhang, and Y. Ye, "On approximating complex quadratic optimization problems via semidefinite programming relaxations," *Mathematical Programming*, vol. 110, no. 1, pp. 93–110, 2007.

[20] A. Subhash, A. Kammoun, A. Elzanaty, S. Kalyani, Y. H. Al-Badarneh, and M.-S. Alouini, "Optimal phase shift design for fair allocation in RIS-aided uplink network using statistical CSI," *IEEE Journal on Selected Areas in Communications*, vol. 41, no. 8, pp. 2461–2475, 2023.